

Preparation and Characterizations of Monocrystalline Na Doped NiO Thin Films

Yacine Aoun^a, Massilia Marrakchi^b, Said Benramache^{a*}, Boubaker Benhaoua^c, Said Lakel^b,
Azzeddine Cheraf^b

^aLaboratoire de Physique Photonique et Nanomatériaux Multifonctionnels, LPPNM, Biskra University, 07000, Biskra, Algeria

^bMaterial Science Department, Faculty of Science, Biskra University, 07000, Biskra, Algeria

^cUnité de Recherche en Energies Renouvelables en zones arides, 39000, El-Oued, Algeria

Received: July 24, 2017; Revised: November 27, 2017; Accepted: December 18, 2017

In the present work, the effect of Na doping on optical, structural and electrical properties of Na doped NiO thin films were studied. The spray pneumatic method was used to deposit the Na doped NiO thin films in the range 0 to 5 wt.%, it are investigated at a substrate temperature of 420 °C with NiO solution 0.1 M. Firstly in the XRD spectra, as found that a only (111) peak was observed for Na doped NiO thin film indicate that the Na doped NiO thin films a monocrystalline in nature with cubic structure. The maximum crystallite size of Na doped NiO thin films was 18.90 nm at 3 wt.%. Secondary, the optical transmissions spectra Na doped NiO thin films having a high transparency with comparing to undoped film in visible region. The band gap energy was decreased after doping by Na and reaching a minimum value is 3.53 eV at 2 wt.%. The minimum value of Urbach energy was 0.312 eV, it is obtained at 3 wt.%. In the end, the minimum electrical resistance of the Na doped NiO films was located at 5 wt.%. The optimum Na doping amount is achieved at 3 at %.

Keywords: NiO, Thin films, Na doping, TCO, Spray pneumatic method.

1. Introduction

Nickel oxide (NiO) is one of the most important oxide materials due to its excellent chemical stability and durability, low toxicity, large span optical density, low cost and good thermal stability¹. There are several reports on deposition of NiO thin films were found by various techniques such as Sol-Gel methods, sputtering, chemical vapor deposition and spray pyrolysis techniques²⁻⁶.

NiO is considered to be a model p-type semiconductor of semiconducting material with large a direct band gap (3.4–4eV)⁷. However, in the past years, NiO was used as a gas sensing due to their high optical transparency and good electrical conductivity. So for, NiO have been widely investigated as thin films for optoelectronic and photovoltaic applications such as sensors⁸, fuel cell electrodes⁹, catalysis¹⁰, thermoelectric devices¹¹, and dye-sensitized solar cells (DSSCs)¹² and electrochromic material for displays¹³.

Wu Chia-Ching and Yang Cheng-Fu¹⁴ investigated the effect of Li doping on structural, optical and electrical properties of Li doped NiO thin films by spray pyrolysis technique. As a results, they found that the Li doped NiO thin films with 8 at.% having a good transparency about 76 % in the visible region, and this film have p-type resistivity of $4.1 \times 10^{-1} \Omega$ with (111) preferred orientation.

The main objective of this work is to obtain a semiconductor as Na doped NiO thin films with high crystalline structure,

good optical and electrical properties. In this work, we have studied the Na effect on structural, optical and electrical properties of NiO thin films, the films were elaborated on glass substrate by using spray pneumatic method at 420 °C for 2 ml/min of deposition rate.

2. Experimental Procedure

2.1 Preparation of spray solution

NiO:Na solutions were prepared by dissolving 0.1M nickel chloride hexahydrate (NiCl₂, 6H₂O) and x wt.% of sodium chloride dehydrate (NaCl, 2H₂O) with the ratio of Na/Ni = 0, 0.02, 0.03, 0.04 and 0.05. The mixtures were dissolved in the solvent containing equal volumes absolute ethanol solution (99.995%) purity, and then have added a some drops of HCl solution as a stabilized, the mixture solution was stirred at 50 °C for 120 min to yield a clear and transparency solution.

2.2 Deposition of thin films

The NiO:Na solutions were sprayed on the heated glass substrates by spray pneumatic method which transforms the liquid to a stream formed with uniform and fine droplets of 25 μm average diameter. The deposition was performed at a substrate temperature of 420 °C with deposition rate was 2 mL/ min. The prepared NiO:Na films at different Na doping levels are 0 wt.%, 2 wt.%, 3 wt.%, 4 wt.%, and 5 wt.%.

*e-mail: benramache.said@gmail.com.

2.3 Characterization

The structural properties of Na doped NiO films were studied by means of X-ray diffraction (XRD Bruker AXS-8D) with CuK α radiation ($\lambda = 0.15406$ nm) in the scanning range of (2θ) was between 20° and 50° . The optical transmission of the deposited films was measured in the range of 300-1000 nm by using an ultraviolet-visible spectrophotometer (LAMBDA 25) and the electrical resistance R was measured by four point methods.

3. Results and Discussion

3.1 Effect of Na doping on crystalline structure

We have reported in Figure 1, the spectra's of X-ray diffraction of Na doped NiO thin films at different Na doping levels. The XRD spectrum of the product revealed that the structure of NiO thin films is cubic structure (JCPDS) No. 73- 1519)¹⁵. However, there is one diffraction peak was detected in all spectra's at $2\theta = 37.3^\circ$, which is (111) phase related to NiO phase, so that the Na doped NiO thin films is monocrystalline nature. As shown in the Figure 1, the intensities of (111) peak in Na doped NiO thin films was decreased after doping. From Table 1 show that the diffraction angle of (111) peak also was decreased after doping by Na due to the atomic rayon of Na, the shift to lower angles of (111) peak after doping has been indicated by the enhancement of the crystallinity with a-axis orientation. The optimum result can be observed with doped films at 2 and 3 wt.%.

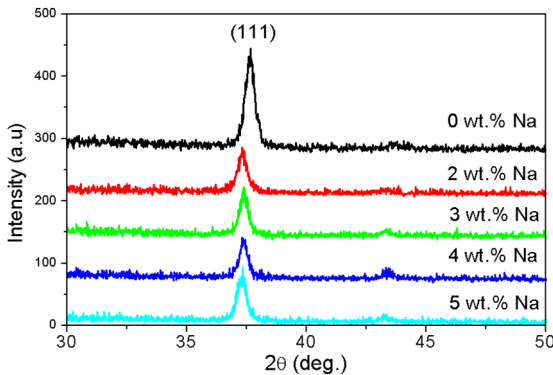


Figure 1. X-ray diffraction spectra of Na doped NiO thin films with various doping levels.

Table 1. The measurements of Bragg angle 2θ , the full width at half-maximum FWHM, the crystallite size G , lattice parameter a and $a_0 - a$ of (111) diffraction peak for Na doped NiO thin films with doping level.

Na Doping (wt.%)	2θ (deg)	β (rad)	G (nm)	a (nm)	$a_0 - a$ (nm)
0	37.645	0.00889	16.47	0.41385093	0.00374907
2	37.321	0.00885	16.53	0.41731416	0.00028584
3	37.386	0.00774	18.90	0.41661447	0.00098553
4	37.378	0.00787	18.61	0.41670045	0.00089955
5	37.300	0.00866	16.91	0.41754074	5.9259E-05

The crystalline structure information was defined by the interplanar distance, it is determined by the position of the Bragg peaks, is a discontinuous function of the Miller indices ($h k l$), which identify the crystallographic planes. The lattice parameter a of Na doped NiO thin films was calculated from XRD patterns by using the following equation⁴:

$$d_{(hkl)} = \frac{a}{\sqrt{(h^2 + k^2 + l^2)}} \quad (1)$$

where d_{hkl} is the interplanar spacing, h, k and l are the mille indices of the planes and a is the lattice parameter of (111) plane.

Figure 2, shows the variation of $a_0 - a$ of (111) peak of Na doped NiO thin films as a function of doping level. As seen in Figure 2, this variation is high than zero and decreased with increasing the Na doping, which was found that the lattice parameter of Na doped NiO thin films is smaller than the undoped film. From Table 1 can observed that the $a_0 - a$ of (111) was decreased after doping by Na, which can be explained by the decrease in the defects.

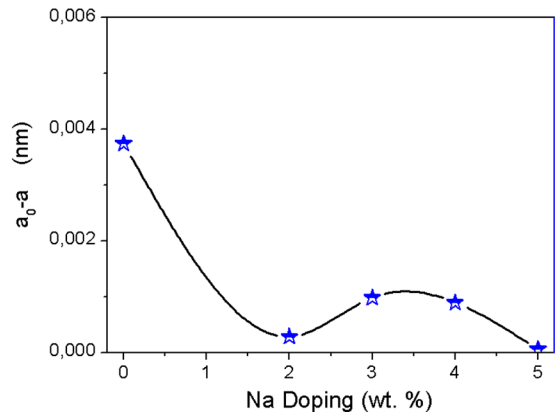


Figure 2. The Variation of $a_0 - a$ of (111) peak in Na doped NiO thin films as a function of doping level.

In order to study the crystalline structure, the crystallite size G of (111) plane was calculated by the full width at half-maximum (FWHM) and diffraction peak of (111) plane of Na doped NiO films, as calculated by Scherer's equation¹⁶:

$$G = \frac{0.9\lambda}{\beta \cos \theta} \quad (2)$$

where G is the crystallite size, λ is the wavelength of X-ray ($\lambda = 1.5406 \text{ \AA}$), β is the full width at half-maximum (FWHM), and θ is angle of diffraction peak. The crystallite sizes values and FWHM are illustrated in Table 1 as a function of Na doping level.

In Figure 3, we reported the variation of crystallite size of Na doped NiO thin films as a function of Na doping level, as seen that the crystallite size of NiO thin films was increased after doping by Na from 16.47 to 18.90 nm, when the Na concentration increase from 0 to 3 wt.%, after this point, we have found that the crystallite size to be decreased to 16.91 at 5 wt.%. The increase in the crystallite size of Na doped NiO thin films can be explained by the enhancement of crystalline structure of Na doped NiO thin films, but the decrease of crystallite size of Na doped NiO thin films with decreasing of a_0 - a variation (see Figure 2) can be related to improve of electrical characterizations of Na doped NiO thin films.

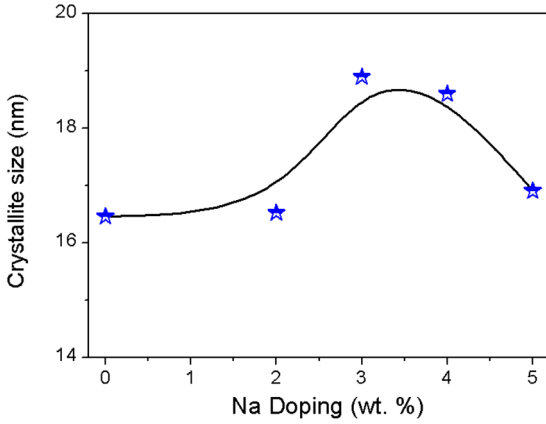


Figure 3. The variation of crystallite size of (111) peak in Na doped NiO thin films at different doping levels.

3.2 Effect of Na doping on optical properties

The effect of Na doping on optical property is shown in Figure 4, we reported the optical transmission spectra of Na doped NiO thin films as a function of Na doping level. As shown that the optical transmission of Na doped NiO thin films are improved after doping by Na. As can be seen, the transmission of Na doped NiO thin films is varied between 35 to 60 % in the visible region. The increase in transmission of Na doped NiO thin films in the visible region can be explained by the increase in crystallite size in this region (see Figure 3) as expressed as¹⁷. The region of absorption edge was located between 360-300 nm in the layers, it is a region of transition between the valence band and the conduction band.

The optical property information was based on calculate of band gap energy E_g , it is determined by the transmission spectra which is transforms the all points to the absorbance according to the following equations¹⁸:

$$A = \alpha d = -\ln T \quad (3)$$

$$(Ah\nu)^2 = B(h\nu - E_g) \quad (4)$$

where A is the absorbance, d is the film thickness; T is the transmission spectra of thin films; α is the absorption coefficient values; B is a constant, $h\nu$ is the photon energy and E_g the band gap energy of Na doped NiO thin films.

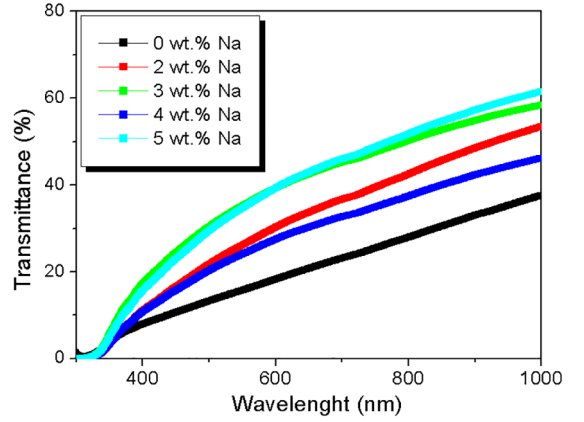


Figure 4. The transmission spectra of Na doped NiO thin films as a function of doping level.

One can estimate the optical gap (E_g) starting from the extrapolation of the curve which presents the evolution of $(Ah\nu)^2$ as a function of $h\nu$. The intersection of the linear region on the $h\nu$ axis gives the E_g . As shown in Figure 5a, the same thing as the optical gap. The Urbach energy (E_u) is related to the disorder in the film network, as it is expressed follow¹⁹:

$$A = A_0 \exp\left(\frac{h\nu}{E_u}\right) \quad (5)$$

where A_0 is a constant, $h\nu$ is the photon energy and E_u is the Urbach energy, it is presented in Table 2. The Figure 5b shows the drawn of $\ln A$ as a function of photon energy $h\nu$ for deduce the Urbach energy. We have obtained these curves for each different film.

Figure 6 shows the variation of the optical band gap energy E_g and the Urbach energy E_u of Na doped NiO thin films at different Na doping levels. As clearly seen, the variation of optical gap energy of Na doped NiO thin films was decreased after doping by Na at 2 wt.%, this is confirming that the electrical property was improved. The minimum value of optical band gap energy was obtained in the Na doped NiO thin film with 2 wt.% it is 3.53 eV. But, 5 wt.% have an optical energy highest one it is 3.64 eV, this is related to film thickness in this point. However, the Na doped NiO thin films having a few defect with minimum value of Urbach energy, it is decreased after doping, the minimum was found at 3 wt.% of 0,312 eV.

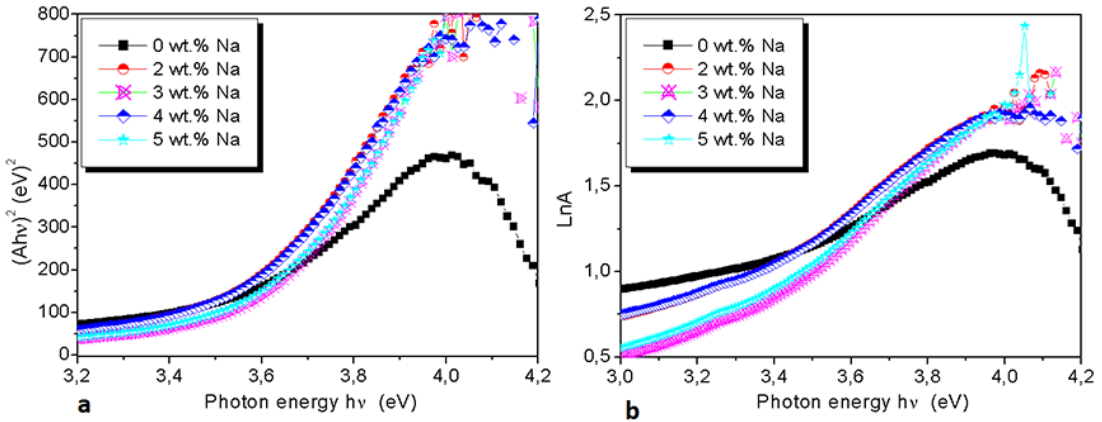


Figure 5. a. The typical variation of $(Ahv)^2$ vs. photon energy hv for Na doped NiO thin films; b. The drawn of $\ln A$ as a function of photon energy (hv) for deduce the Urbach energy for Na doped NiO thin films.

Table 2. The variation of band gap energy E_g and the Urbach energy E_u of Na doped NiO thin films as a function of doping level.

Na Doping (wt.%)	E_g (eV)	E_u (meV)
0	3.62	0.422
2	3.53	0,357
3	3.60	0,312
4	3.54	0,352
5	3.64	0,329

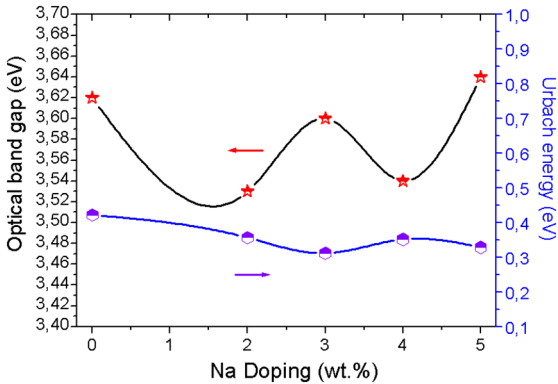


Figure 6. The variation of optical band gap and Urbach energy of Na doped NiO thin films as a function of doping level.

3.3 Effect of Na doping on the electrical properties

In the final description of obtain results, Figure 7 show the variation of electrical resistance R_{sh} of Na doped NiO films as a function of Na doping level. It was determined by following formula:

$$R_{sh} = \frac{\pi}{\ln(2)} \cdot \frac{V}{I} \quad (6)$$

where I is the applied current = $0.5 \cdot 10^{-6}$ and V is the measurement voltage. As can be seen, the electrical resistance of NiO films was decreased after doping by Na

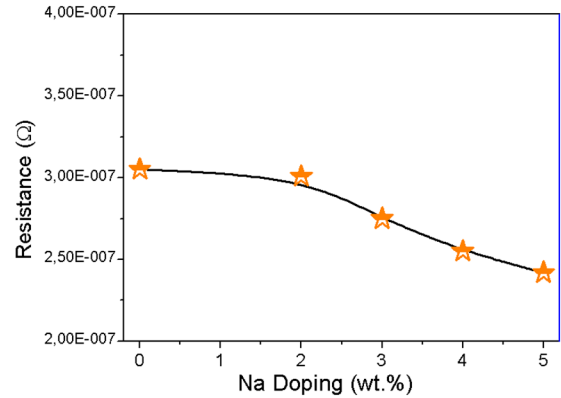


Figure 7. The Electrical resistance variation of Na doped NiO thin films as a function of doping level.

in all deposited films; this decrease can be explained by the increase of crystallite size (see Figure 3). The decreases of the electrical resistance with increasing of the Na doping can be explained by increasing of the oxygen vacancy.

4. Conclusion

In this work, we have studied the effect of Na doping on crystal structure, optical and electrical properties of NiO thin films. The following results were obtained:

- As found that a only (111) peak was observed for Na doped NiO thin film indicate that the Na doped NiO thin films a monocrystalline in nature with cubic structure.
- The maximum crystallite size of Na doped NiO thin films was 18.90 nm at 3 wt.%.
- The optical transmissions spectra showed all samples of Na doped NiO thin films having a transparency high than the undoped in visible region.
- The band gap energy was decreased after doping by Na and reaching a minimum value is 3.53 eV at 2 wt.%.

- The minimum value of Urbach energy was 0.312 eV, it is obtained at 3 wt.%.
- The minimum electrical resistance of the NiO films was located at 5 wt.%.
- The best estimated structure, optical and electrical characterizations are achieved for sprayed Na doped NiO thin films at 3 wt.%.

5. References

1. Gao H, Gao D, Zhang J, Zhang Z, Yang G, Shi Z, et al. Synthesis and anomalous magnetic behaviour of NiO nanotubes and nanoparticles. *IET Micro & Nano Letters*. 2012;7(1):5-8.
2. Nam KW, Yoon WS, Kim KB. X-ray absorption spectroscopy studies of nickel oxide thin film electrodes for supercapacitors. *Electrochimica Acta*. 2002;47(19):3201-3209.
3. Stamataki M, Tsamakidis D, Brilis N, Fasaki I, Giannoudakos A, Kompitsas M. Hydrogen gas sensors based on PLD grown NiO thin film structures. *Physica Status Solid (A)*. 2008;205(8):2064-2068.
4. Dendouga S, Benramache S, Lakel S. Influence of Film Thickness on Optical and Electrical Properties of Nickel Oxide (NiO) Thin Films. *Journal of Chemistry and Materials Research*. 2016;5(4):78-84.
5. Tenent RC, Gillaspie DT, Miedaner A, Parilla PA, Curtis CJ, Dillon AC. Fast-Switching Electrochromic Li⁺-Doped NiO Films by Ultrasonic Spray Deposition. *Journal of the Electrochemical Society*. 2010;157(3):H318-H322.
6. Korošec RC, Bukovec P. Sol-Gel Prepared NiO Thin Films for Electrochromic Applications. *Acta Chimica Slovenica*. 2006;53(2):136-147.
7. Hotovy I, Spiess L, Predanocny M, Rehacek V, Racko J. Sputtered nanocrystalline NiO thin films for very low ethanol detection. *Vacuum*. 2014;107:129-131.
8. Zhao S, Shen Y, Zhou P, Zhang J, Zhang W, Chen X, et al. Highly selective NO₂ sensor based on p-type nanocrystalline NiO thin films prepared by sol-gel dip coating. *Ceramics International*. 2018;44(1):753-759.
9. Zhang P, Ma X, Wang K, Tao Z, Liu T, Yang L. Synthesis of hierarchical structured flower-like Ni(OH)₂ and NiO and their application in waste water treatment. *IET Micro & Nano Letters*. 2012;7(6):505-507.
10. Qiu Y, Yu J, Tan C, Zhou X, Yin J. Synthesis of a novel NiO tube with porous surface constructed by nanoworms. *IET Micro & Nano Letters*. 2012;7(1):56-59.
11. Sajjal K, Raj AME. Effect of thickness on structural and magnetic properties of NiO thin films prepared by chemical spray pyrolysis (CSP) technique. *Materials Letters*. 2016;164:547-550.
12. Wang N, Liu CQ, Wen B, Wang HL, Liu SM, Chai WP. Enhanced optical and electrical properties of NiO thin films prepared by rapid radiation pyrolysis method based on the sol-gel technique. *Materials Letters*. 2014;122:269-272.
13. Mallick P, Rath C, Prakash J, Mishra DK, Choudhary RJ, Phase DM, et al. Swift heavy ion irradiation induced modification of the microstructure of NiO thin films. *Nuclear Instruments and Methods in Physics Research Section B: Beam Interactions with Materials and Atoms*. 2010;268(10):1613-1617.
14. Wu CC, Yang CF. Investigation of the properties of nanostructured Li-doped NiO films using the modified spray pyrolysis method. *Nanoscale Research Letters*. 2013;8:33.
15. Patil PS, Kadam LD. Preparation and characterization of spray pyrolyzed nickel oxide (NiO) thin films. *Applied Surface Science*. 2002;199(1-4):211-221.
16. Benramache S, Benhaoua B. Influence of substrate temperature and Cobalt concentration on structural and optical properties of ZnO thin films prepared by Ultrasonic spray technique. *Superlattices and Microstructures*. 2012;52(4):807-815.
17. Benramache S, Benhaoua B. Influence of annealing temperature on structural and optical properties of ZnO: In thin films prepared by ultrasonic spray technique. *Superlattices and Microstructures*. 2012;52(6):1062-1070.
18. Benramache S, Benhaoua B, Khechai N, Chabane F. Elaboration and characterisation of ZnO thin films. *Matériaux & Techniques*. 2012;100(6-7):573-580.
19. Benramache S, Aouassa M. Preparation and Characterization of p-Type Semiconducting NiO Thin Films Deposited by Sol-Gel Technique. *Journal of Chemistry and Materials Research*. 2016;5(6):119-122.